KJPP

Original Article

Lyso-globotriaosylsphingosine induces endothelial dysfunction *via* autophagy-dependent regulation of necroptosis

Ae-Rang Hwang[1], Seonghee Park[2,*], and Chang-Hoon Woo[1,*]

[1]Department of Pharmacology, Yeungnam University College of Medicine, Daegu 42415, [2]Department of Physiology, Ewha Womans University College of Medicine, Seoul 07084, Korea

*Correspondence
Seonghee Park
E-mail: sp@ewha.ac.kr
Chang-Hoon Woo
E-mail: changhoon_woo@yu.ac.kr

ABSTRACT Fabry disease is a lysosomal storage disorder characterized by the lysosomal accumulations of glycosphingolipids in a variety of cytotypes, which include endothelial cells. The disease is inherited and originates from an error in glycosphingolipid catabolism caused by insufficient α-galactosidase A activity, which causes uncontrolled progressive storage of intracellular globotriaosylceramide (Gb3) in the vasculature and extracellular accumulation of lyso-Gb3 (a deacetylated soluble form of Gb3). Necrosis can lead to inflammation, which exacerbates necrosis and creates a positive feedback loop that triggers necroinflammation. However, the role played by necroptosis, a form of programmed necrotic cell death, in the cell-to-cell inflammatory reaction between epithelial and endothelial cells is unclear. Thus, the present study was undertaken to determine whether lyso-Gb3 induces necroptosis and whether necroptosis inhibition protects endothelial dysfunction against lyso-Gb3 inflamed retinal pigment epithelial cells. We found lyso-Gb3 induced necroptosis of a retinal pigment epithelial cell line (ARPE-19) in an autophagy-dependent manner and that conditioned media (CM) from ARPE-19 cells treated with lyso-Gb3 induced the necroptosis, inflammation, and senescence of human umbilical vein endothelial cells. In addition, a pharmacological study showed CM from lyso-Gb3 treated ARPE-19 cells induced endothelial necroptosis, inflammation, and senescence were significantly inhibited by an autophagy inhibitor (3-MA) and by two necroptosis inhibitors (necrostatin and GSK-872), respectively. These results demonstrate lyso-Gb3 induces necroptosis via autophagy and suggest that lyso-Gb3 inflamed retinal pigment epithelial cells trigger endothelial dysfunction *via* the autophagy-dependent necroptosis pathway. This study suggests the involvement of a novel autophagy-dependent necroptosis pathway in the regulation of endothelial dysfunction in Fabry disease.

INTRODUCTION

Fabry disease (FD) is an X-linked lysosomal storage disorder caused by the lack of or diminished activities of alpha-galactosidase A (α-gal A; a lysosomal enzyme) [1]. α-Gal A deficiency causes the systemic lysosomal accumulation of glycolipids, predominantly globotriaosylsphingosine (Gb3), and induces vascular endothelial dysfunction [2]. Lyso-Gb3 is the hydrophilic deacyl-

ated form of Gb3 and is detected at high levels in the plasma of FD patients. Gb3 accumulates inside cells and has been suggested to cause autophagy, but the pathological implications of Gb3 accumulation are unclear.

Autophagy is an evolutionarily conserved catabolic process in eukaryotic cells that is critical for maintaining cellular homeostasis and involves the degradation and recycling of cytoplasmic proteins, damaged organelles, and other cellular constituents

[3]. This degradation pathway removes cytoplasmic materials and surrounds cellular components for degradation and begins with the formation of a double-membrane structure called an autophagosome. Autophagosomes then fuse with a lysosome to form an autolysosome, in which lysosome hydrolases degrade the sequestered contents of autophagosomes [1]. However, the role of autophagy in the development of endothelial dysfunction and vascular complications in FD patients has yet to be established.

Necroptosis is a type of programmed necrotic cell death that has unique morphological features with apoptosis and necrosis depending on receptor-interacting serine/threonine-protein kinase 3 (RIPK3, also known as RIP3). Necroptosis is implicated in the pathogeneses of several diseases, including atherosclerosis, myocardial infarction, and pancreatitis, and involved in acute kidney injury and stroke [2]. Lysosomal deposits may act as damage-associated molecular patterns (DAMPs) or cause DAMP production by injured cells, which leads to pro-inflammatory activity because the addition of Gb3 to normal control cells reportedly induces cytokine secretion and apoptosis [4]. Furthermore, there is strong evidence that necroptosis is involved in the initiation and amplification of inflammatory responses in acute and chronic inflammatory disorders [5]. Among lysosomal storage diseases, RIP3 has been linked to the pathogeneses of Gaucher's disease and Niemann–Pick disease [6]. However, the roles of RIP1 and RIP3 in FD have not been elucidated.

Recently, it was shown that necroptosis and inflammatory activation of the innate immune system are general responses in FD and are primarily caused by accumulations of the glycolipids Gb3 and lyso-Gb3, which constitute a recognized danger signal [6]. Due to continuous exposure to glycolipids, inflammation in FD is chronic, and it is possible that tissue necroptosis progresses independently after initial inflammation. Evidence suggests that cellular senescence (characterized by cell cycle arrest and proinflammatory changes in gene expressions) occurs in endothelial cells *in vivo* and may play a role in age-related vascular pathologies like atherosclerosis [7]. However, the cellular and molecular mechanisms that link the intracellular accumulations of substrates such as Gb3 to endothelial senescence, inflammation, and necroptosis are not entirely understood. Therefore, in this study, we investigated the mechanism responsible for lyso-Gb3 induced necroptosis *via* autophagy and for the triggering of endothelial dysfunction by lyso-Gb3 inflamed retinal pigment epithelial cells *via* an autophagy-dependent necroptosis pathway.

METHODS

Reagents and antibodies

Lyso-Gb3 (lyso-Ceramide trihexoside) was purchased from Matreya, LLC. Necrostatin (a RIP1 inhibitor) was purchased from Selleckchem. 3-methyladenine (3-MA, an autophagy inhibitor) and dimethyl sulfoxide were supplied by Sigma. GSK-872 (a RIP3 inhibitor) were obtained from MedChemExpress. Antibodies were purchased from the following vendors, as follows: VCAM-1, ICAM-1, and RIP3 (Santa Cruz Delaware); MLKL (Millipore); LC3 and beclin-1 (Cell Signaling Technology); RIP1 (Invitrogen); and α-tubulin (Sigma).

Cell culture and treatment conditions

ARPE-19 cells (ATCC CRL-2302), a human retinal pigment epithelial cell line, were maintained in DMEM/F12 medium (Lonza) supplemented with 10% fetal bovine serum (FBS) (Gibco-Life Technologies), 50 U/ml penicillin, and 50 μg/ml streptomycin at 37°C in a 95% air-5% CO_2 atmosphere. Cells were cultured for 24 h, pretreated with 3-MA (10 mM), GSK'872 (30 μM), or necrostatin (30 μM), and stimulated with lyso-Gb3 (0.5 μM) for 24 h. Cells were harvested at the indicated time points. Human umbilical vein endothelial cells (HUVECs) were cultured in 0.2% gelatin-coated cell culture dishes in M200 medium (Gibco) containing 5% FBS and endothelial growth factor supplement (LSGS; Cascade biologics). Cells were used for experiments at passages 4, 5, or 6. Morphological changes were observed under a light microscope at ×100.

Western blot analysis

Cells were lysed in radioimmunoprecipitation assay lysis buffer supplemented with 1 mM phenylmethylsulfonyl fluoride and 0.01 mM protease inhibitor cocktail (Roche) and lysates were incubated on ice for 15 min and centrifuged at $15,000 \times g$ for 10 min at 4°C. Protein concentrations were determined using a Bradford assay (Bio-Rad). Proteins were separated by SDS-PAGE and transferred to polyvinylidene difluoride membranes, followed by immunoblotting with primary antibodies (1:1,000 dilution) and corresponding secondary antibodies (1:4,000 dilution). Signals were visualized using electrochemiluminescence detection reagents (Millipore), according to the manufacturer's instructions.

MLKL oligomerization

Non-reducing SDS/PAGE is carried out as regular SDS/PAGE, except that cell lysates were mixed with SDS sampling buffer without the reducing agent 2-Mercaptoethanol. MLKL oligomers were analyzed by non-reducing SDS/PAGE followed by Western blotting with anti-MLKL antibody.

Real time quantitative reverse transcriptase polymerase chain reaction (qRT-PCR)

The mRNA expressions of genes were determined by qRT-PCR as described previously [8]. Briefly, total amount of RNA was isolated with easy-BLUE (iNtRON), and reverse transcription was

performed using TaqMan reverse transcription reagents according to the manufacturer's instructions. qRT-PCR was performed on Power SYBR Green in an ABI PRISM 7500 unit using 1 μl of template cDNA. Quantification was performed using the efficiency-corrected ΔΔCq method.

The primers used to amplify DNA sequences were as follows: RIP1 forward 5'-GCCCAACCGCGCTGAGTACA-3' and reverse 5'-TGCCTTCTATGGCCTCCACGA-3' RIP3 forward 5'-TGTCAAGTTATGGCCTACTGGTGCG-3' and reverse 5'-AACCATAGCCTTCACCTCCCAGGAT-3' MLKL forward 5'-GGATTGCCCTGAGTTGTTGC-3' and reverse 5'-AACCGCAGACAGTCTCTCCA-3'

PCR conditions were as follows: preliminary denaturation at 50°C for 2 min, followed by 95°C for 10 min, 95°C for 15 sec, and 60°C for 1 min.

Immunofluorescence analysis

ARPE-19 cells were fixed with 4% buffered paraformaldehyde for 1 h, permeabilized with 0.2% Triton X-100 for 5 min at room temperature (RT), blocked with 5% normal goat serum in PBS-0.05% Tween 20, and incubated with anti-LC3B antibody (1:100) overnight at 4°C. Cells were then treated with Alexa Fluor 488 goat anti-rabbit secondary antibody at 1:200 (Invitrogen) for 1 h at RT. Nuclei were stained with DAPI for 30 min at RT, and cells were observed under a K1-Fluo confocal laser scanning microscope (Nanoscope Systems).

Senescence-associated β-galactosidase (SA-β-gal) staining

SA-β-gal staining was performed as previously described [9]. Briefly, HUVECs were seeded on 6-well plates, fixed with 4% formaldehyde at RT for 1 h, washed with PBS, and then stained using a SA-β-gal staining Kit (Sigma-Aldrich). The ratio of blue positive cells per 100 cells were measured by calculating under a light microscope at ×200.

Enzyme-linked immunosorbent assay (ELISA)

ARPE-19 cells were cultured in 6 well plates until 80%–90% confluent. After removing the growth medium, the cells were incubated overnight in a serum-free ARPE-19 medium. Cells were pretreated with 3-MA for 1 h and then stimulated with Lyso-Gb3 for 24 h. The conditioned medium was collected and centrifuged at $3,000 \times g$ for 10 min to eliminate cell debris. The levels of interleukin (IL)-1β, interferon gamma (IFN-γ), tumor necrosis factor α (TNF-α), and IL-6 secreted in the conditioned medium were determined using a human proinflammatory cytokine multiplex ELISA kit (arigo Biolaboratories) according to the manufacturer's instructions.

Transmission electron microscopy (TEM)

ARPE-19 cells were plated in 6 wells and one day later when ~70% confluent cells were exposed to lyso-Gb3 (0.5 μM) in fresh medium without antibiotics for 24 h. After fixation, subsequent procedures were conducted as previously described [10]. For TEM studies, cell pellets were washed with PBS three times, fixed in 0.1 M sodium cacodylate (NaCac) buffer (pH 7.4) containing 2% glutaraldehyde, post-fixed in 0.1 M NaCac containing 2% osmium tetroxide, stained en bloc with 2% uranyl acetate, dehydrated using a graded ethanol series, embedded in Epon-Araldite resin, sectioned with a diamond knife, and stained with uranyl acetate and lead citrate. Cells were observed using a transmission electron microscope (JEM 1230-JEOL USA Inc.) at 110 kV and imaged with a CCD camera equipped with a first light digital camera controller (Gatan Inc.).

Treatment of HUVECs with conditioned media (CM)

ARPE-19 cells were pretreated with vehicle, necrostatin (30 μM), GSK-872 (30 μM), or 3-MA (10 mM) for 1 h, and then incubated with lyso-Gb3 (0.5 μM) for 3 h. Media were then replaced with fresh medium, and CM were recovered after overnight culture. HUVECs were cultured in CMs for 24 h and then subjected to immunoblotting or cellular senescence assays.

Statistical analysis

Results in bar graphs are presented as means ± SDs. The significances of intergroup differences were assessed by Student's t-test and multiple group comparisons using ANOVA followed by Bonferroni's *post-hoc* test, and p-values of < 0.05 were considered statistically significant. Results are presented as the means of at least three independent experiments.

RESULTS

Lyso-Gb3 induced autophagy in ARPE-19 retinal pigment epithelial cells

Lyso-Gb3 were found to induce autophagy in ARPE-19 cells (a human retinal pigment epithelial cell line). Electron microscopy showed typical vacuolar features of autophagy and fluorescence microscopy revealed puncta formation of LC3 in response to lyso-Gb3 (Fig. 1A, B). We found that lyso-Gb3 induced mixed types of autophay and ER-phagy was a major type of autophagy, suggesting that damaged ER membrane and constituents might be degraded or recycled through autophagy. In addition, lyso-Gb3-induced LC3 puncta formation and LC3B expression were suppressed by 3-MA (an autophagy inhibitor), suggesting lyso-Gb3 induced autophagy in retinal pigment epithelial cells (Fig.
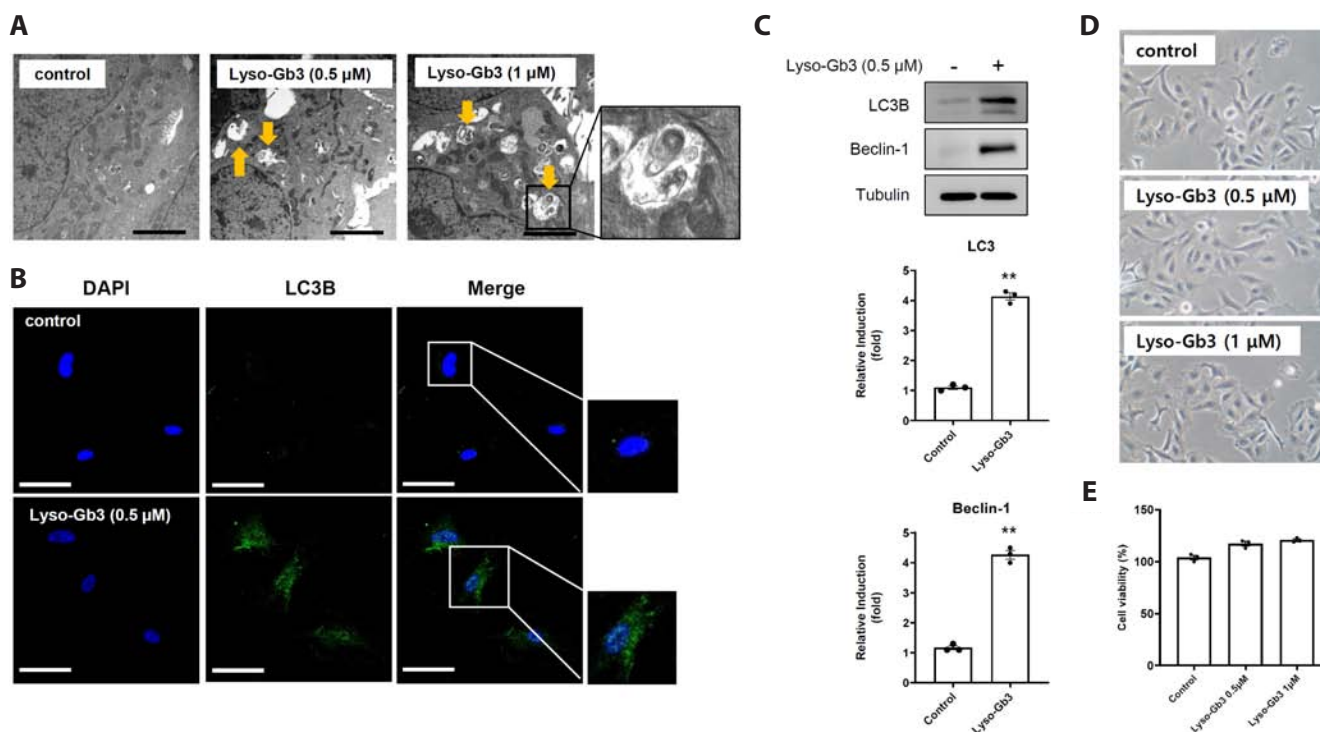
Fig. 1. Lyso-Gb3 induces autophagy in ARPE-19 cells. (A) ARPE-19 cells were exposed to the indicated concentrations of lyso-Gb3 for 24 h. Transmission electron microscopic image of an autophagosome. Scale bar, 1 μm. (B) ARPE-19 cells were pretreated with 3-MA (10 mM) for 1 h and then incubated with lyso-Gb3 (0.5 μM) for 24 h. Autophagy was confirmed by indirect immunofluorescent staining using LC3 antibodies. Nuclei were stained with DAPI. Images were captured at an original magnification of ×600. Scale bar, 50 μm. (C) ARPE-19 cells were exposed to lyso-Gb3 (0.5 μM) for 24 h, and protein expressions were assessed by immunoblotting with anti-LC3B, anti-beclin-1, and anti-tubulin antibodies. Results are representative of three independent experiments. Bar graphs show densitometric quantifications of Western blot bands. (D) Cellular morphologies were observed under a light microscope using the same conditions. (E) Cell viabilities were determined using an MTT assay under the same conditions. Results are representative of three independent experiments. 3-MA, 3-Methyladenine. **p < 0.01 *vs.* vehicle controls, one-way ANOVA followed by Bonferroni's *post-hoc* test.

1B, C). The effects of lyso-Gb3 on ARPE-19 cell viability were determined by MTT analysis. Lyso-Gb3 treatment slightly increased cell viability and similar phenotype was confirmed by morphological analysis under a light microscope (Fig. 1D, E). These results suggest that lyso-Gb3 induced ARPE-19 cell autophagy without affecting cell viability.

Lyso-Gb3 induced necroptosis and inflammation in an autophagy-dependent manner in ARPE-19 cells

Necroptosis is induced by extracellular stimuli and mediated by RIP1, RIP3, and MLKL (mixed lineage kinase domain-like protein). Lyso-Gb3 dose-dependently increased RIP1 and RIP3 as well as phosphorylated levels of MLKL (Fig. 2A). To examine the role of autophagy in the regulation of necroptosis, ARPE-19 cells were exposed to lyso-Gb3 in the presence or absence of 3-MA (an autophagy inhibitor), and expressions of necroptosis-related molecules were then determined by Western blot and quantitative real time PCR. As shown in Fig. 2B, biochemical data showed that 3-MA significantly inhibited the up-regulations of autophagy-related proteins (LC3, beclin-1) and of necroptosis-

associated markers (RIP1, RIP3, MLKL), and we also determined lyso-Gb3-induced MLKL oligomerization in ARPE-19 cells. Under non-reducing conditions, MLKL Western blotting detected the formation of around 250 kDa MLKL oligomers in ARPE-19 cells treated with lyso-Gb3 (Fig. 2C). On the other hand, in the cultures of ARPE-19 cells treated with the autophagy inhibitor 3-MA, low amounts of MLKL oligomers were detected, suggesting that MLKL phosphorylation leads to its oligomerization, creating pores for inflammatory cytokine release. In addition to protein expression, a similar pattern was observed for the mRNAs of RIP1, RIP3, and MLKL (Fig. 2D). Inflammatory cytokines are signaling molecules secreted by immune cells such as helper T cells, macrophages, and other cell types that promote inflammation, including IL-1β, IL-6, IL-12, IL-18, TNF-α, and IFN-γ. The innate immune response is mediated by inflammatory cytokines, which are primarily generated and implicated in the upregulation of the inflammatory response [11,12]. In recent years, it has been evident that inflammation and simultaneous activation of the innate immune system are common responses in FD and arise primarily due to accumulation of glycolipids (Gb3 and Lyso-Gb3), which function as risk signals. Lysosomal deposits have been
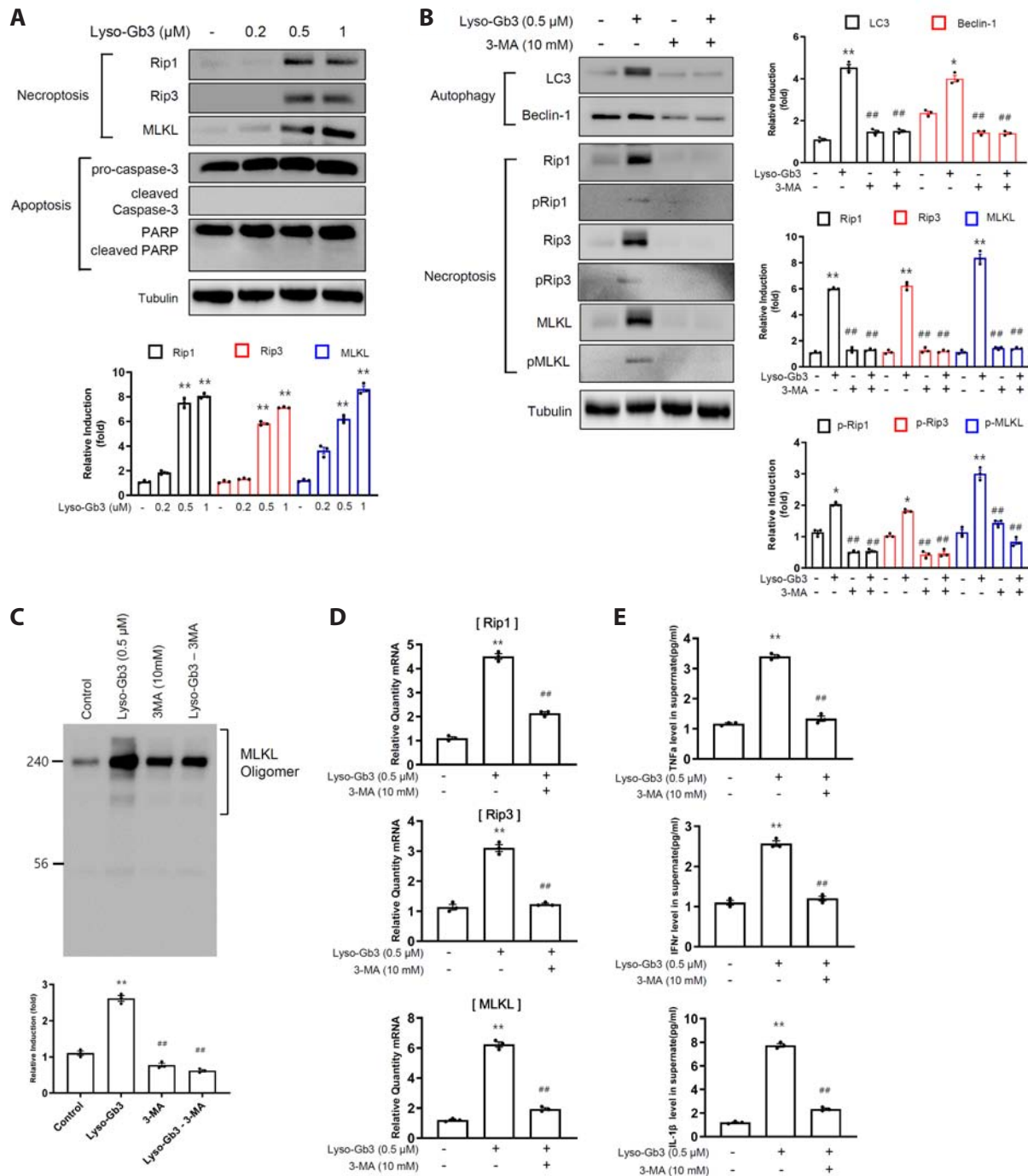
Fig. 2. Lyso-Gb3 induces necroptosis in an autophagy-dependent manner in ARPE-19 cells. (A) ARPE-19 cells were exposed to the indicated concentrations of lyso-Gb3 for 24 h. Protein expressions were determined by immunoblotting with anti-RIP1, anti-RIP3, anti-MLKL, and anti-tubulin antibodies. Bar graphs show densitometric quantifications of Western blot bands. (B) ARPE-19 cells were first incubated with 3-MA (10 mM) for 1 h and then incubated with lyso-Gb3 (0.5 μM) for 24 h. Protein expression was determined by immunoblotting with anti-LC3, anti-beclin-1, anti-RIP1, anti-RIP3, anti-MLKL, and anti-tubulin antibodies. Bar graphs present densitometric quantifications of Western blot bands. (C) ARPE-19 cells were first incubated with 3-MA (10 mM) for 1 h and then incubated with lyso-Gb3 (0.5 μM) for 24 h. The cell lysates were resolved on non-reducing gel and analyzed by immunoblotting with anti-MLKL antibody. (D) The mRNA expressions of RIP1, RIP3, and MLKL were determined by quantitative real time-PCR analysis in ARPE-19 cells treated with lyso-Gb3 in the presence or absence of 3-MA (10 mM). qRT-PCR analysis was performed in triplicate. (E) ELISA assay was conducted to analyze the effect of 3-MA on IL-1β, IFN-γ, and TNF-α secretion by lyso-Gb3. ARPE-19 cells were pretreated with 3-MA (10 mM) for 1 h, followed by 24-h incubation with lyso-Gb3 (0.5 μM). (F) ARPE-19 cells were first incubated with 3-MA (10 mM) for 1 h and then incubated with TNF-α (5 ng/ml), IL-1β (10 ng/ml) and IFN-γ (10 ng/ml) for 24 h. Protein expressions were determined by immunoblotting with anti-RIP1, anti-RIP3, anti-MLKL, and anti-tubulin antibodies. Bar graphs show densitometric quantifications of Western blot bands. The results represent three independent experiments. 3-MA, 3-methyladenine; TNF-α, tumor necrosis factor α; IL, interleukin; IFN-γ, interferon gamma. *$p < 0.05$ and **$p < 0.01$ *vs.* vehicle controls, #$p < 0.05$ and ##$p < 0.01$ *vs.* lyso-Gb3 treated cells and pro-inflammatory cytokine treated cells, one-way ANOVA followed by Bonferroni's *post-hoc* test.
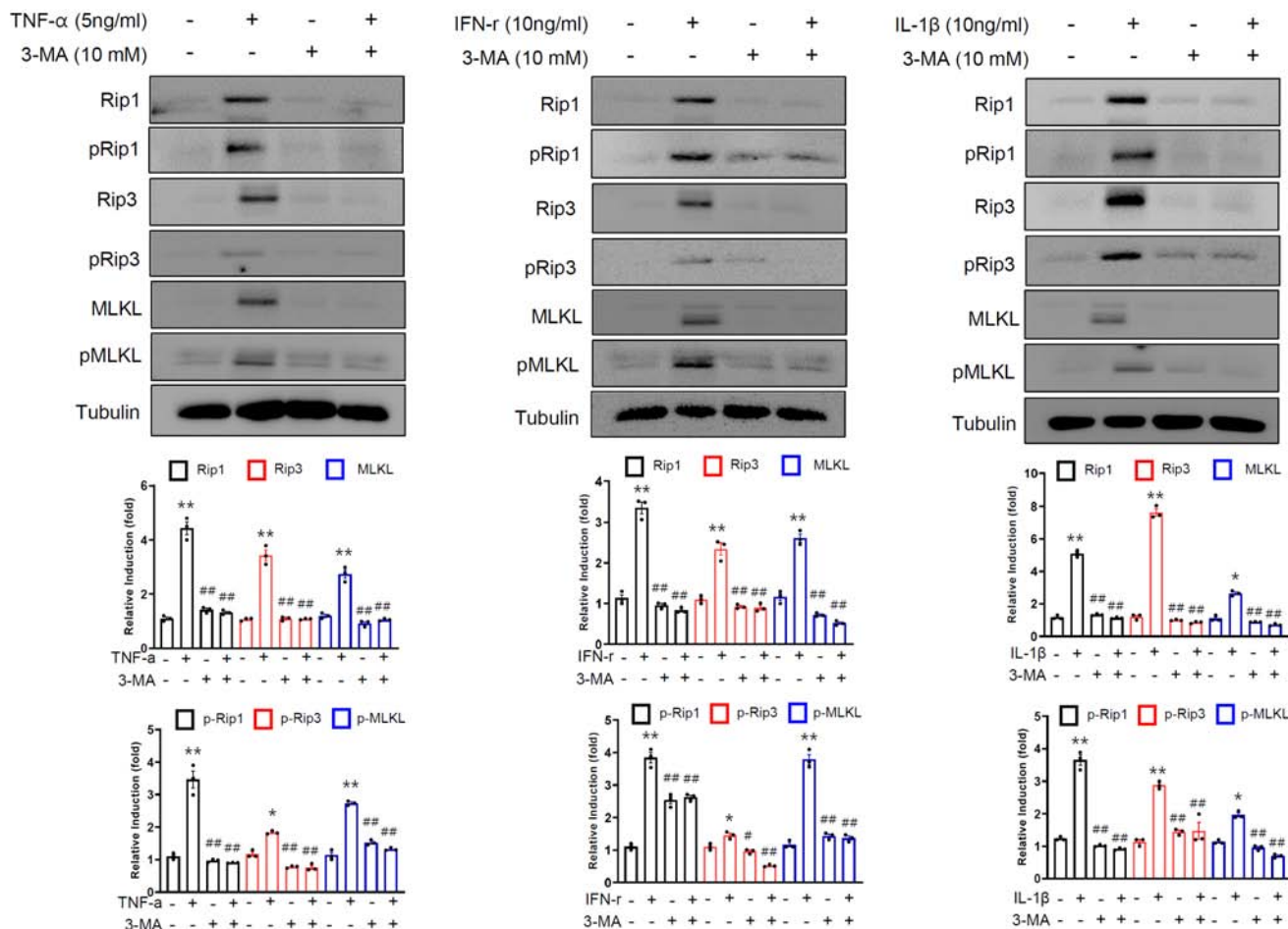
F

Fig. 2. Continued.

shown to induce DAMP production in damaged cells through cell lysis, and the addition of lyso-Gb3 to normal control cells induces cytokine secretion [13-16]. Therefore, to investigate the role of autophagy in the inflammatory response initiation through necroptosis induced by lyso-Gb3, TNF-α, IL-1β and IFN-γ treatment, cells were exposed to autophagy inhibitor 3-MA prior to Lyso-Gb3, TNF-α, IL-1β, and IFN-γ, and the levels of proinflammatory molecules were measured using ELISA and Western blot (Fig. 2E, F). As shown in Fig. 2E, lyso-Gb3 increased the levels of IL-1β, IFN-γ, and TNF-α, whereas 3-MA pretreatment significantly inhibited these upregulations. In addition, 3-MA pretreatment significantly suppressed the protein expressions of necroptosis-related molecules by TNF-α, IL-1β and IFN-γ (Fig. 2F). Taken together, our findings suggest that lyso-Gb3 upregulates necroptosis and inflammation in an autophagy-dependent manner in ARPE-19 cells.

CM from lyso-Gb3 treated ARPE-19 increased endothelial necroptosis and inflammation

We next investigated whether lyso-Gb3 affects RIP1/RIP3/MLKL-induced epithelial necroptosis and inflammation in a cell-autonomous manner or indirectly by secreting molecules into conditioned media, which would indicate the triggering of neighboring endothelial cell necroptosis in a paracrine manner. As shown in Fig. 3A, ARPE-19 cells were pretreated with 30 μM of necrostatin (a RIP1 inhibitor), 30 μM GSK'872 (a specific inhibitor of RIP3), or 10 mM of 3-MA for 1 h, and then incubated with lyso-Gb3 (0.5 μM) for 3 h. Media were then replaced with fresh medium to remove remaining lyso-Gb3. After overnight culture, CM was transferred to HUVECs, and 24 h later, protein levels of necroptosis-associated markers (RIP1, RIP3, MLKL), autophagy-associated markers (LC3B, beclin-1), and inflammation-associated markers (VCAM-1 and ICAM-1) in HUVECs were analyzed by immunoblotting analysis. CM from lyso-Gb3 treated ARPE-19 cells was found to accelerate endothelial necroptosis and inflammation in HUVECs (Fig. 3B), and pretreatment of ARPE-19
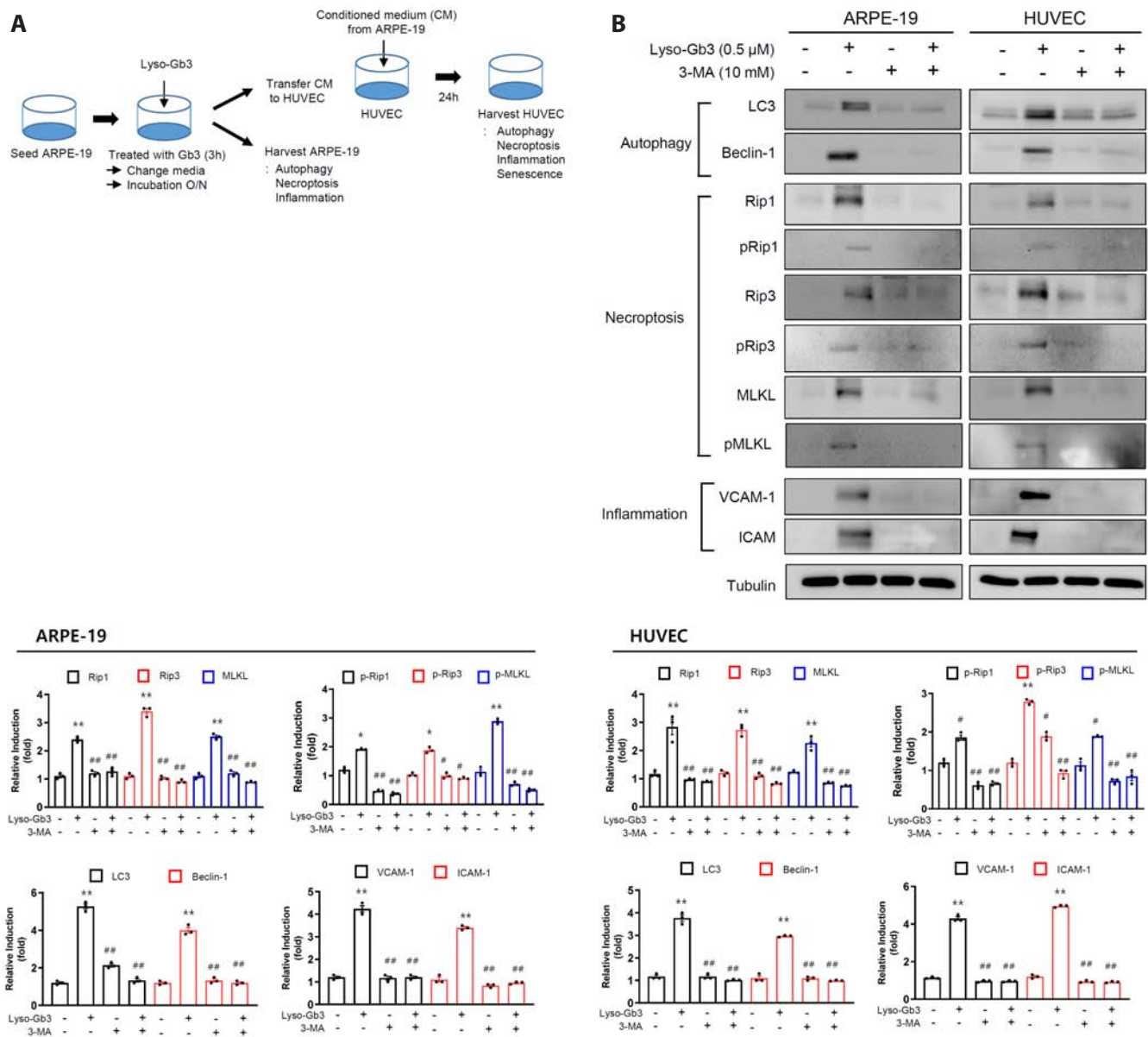
Fig. 3. Conditioned media of lyso-Gb3 treated ARPE-19 cells increases endothelial necroptosis and inflammation. (A) Schematic view of the experiment design. (B–D) ARPE-19 cells were pretreated with necrostatin (30 μM), GSK'872 (30 μM), or 3-MA (10 mM) for 1 h and then incubated with lyso-Gb3 (0.5 μM) for 3 h. Media were then replaced with fresh medium. After overnight (O/N) incubation, the conditioned medium (CM) was recovered and then transferred to HUVECs for further incubation for 24 h. ARPE-19 cells and HUVECs were immunoblotted using anti-RIP1, anti-RIP3, anti-MLKL, anti-LC3, anti-beclin-1, anti-VCAM-1, anti-ICAM-1, and anti-tubulin antibodies. Bar graphs show densitometric quantifications of Western blot bands. 3-MA, 3-methyladenine; HUVEC, human umbilical vein endothelial cell. $*p < 0.05$ and $**p < 0.01$ vs. vehicle controls, $^\#p < 0.05$ and $^{\#\#}p < 0.01$ vs. lyso-Gb3 treated cells, one-way ANOVA followed by Bonferroni's $post$-hoc test.

cells with necrostatin, GSK'872, or 3-MA significantly suppressed CM-induced necroptosis and inflammation in HUVECs treated with CM of lyso-Gb3 treated ARPE-19 cells (Fig. 3B–D). These results showed lyso-Gb3 induced necroptosis via autophagy and that lyso-Gb3 treated retinal pigment epithelial cells could trigger endothelial necroptosis and inflammation via autophagy-dependent necroptosis.

CM of lyso-Gb3 treated ARPE-19 cells increased endothelial senescence

Necroptosis and inflammation are closely associated with cellular senescence, and thus, we investigated whether lyso-Gb3 affects endothelial senescence via autophagy-dependent necroptosis in a paracrine manner. CM of lyso-Gb3 treated ARPE-19 cells induced positive staining by SA-β-gal in a time-dependent manner in HUVECs (Fig. 4A), and pretreatment with necrostatin,
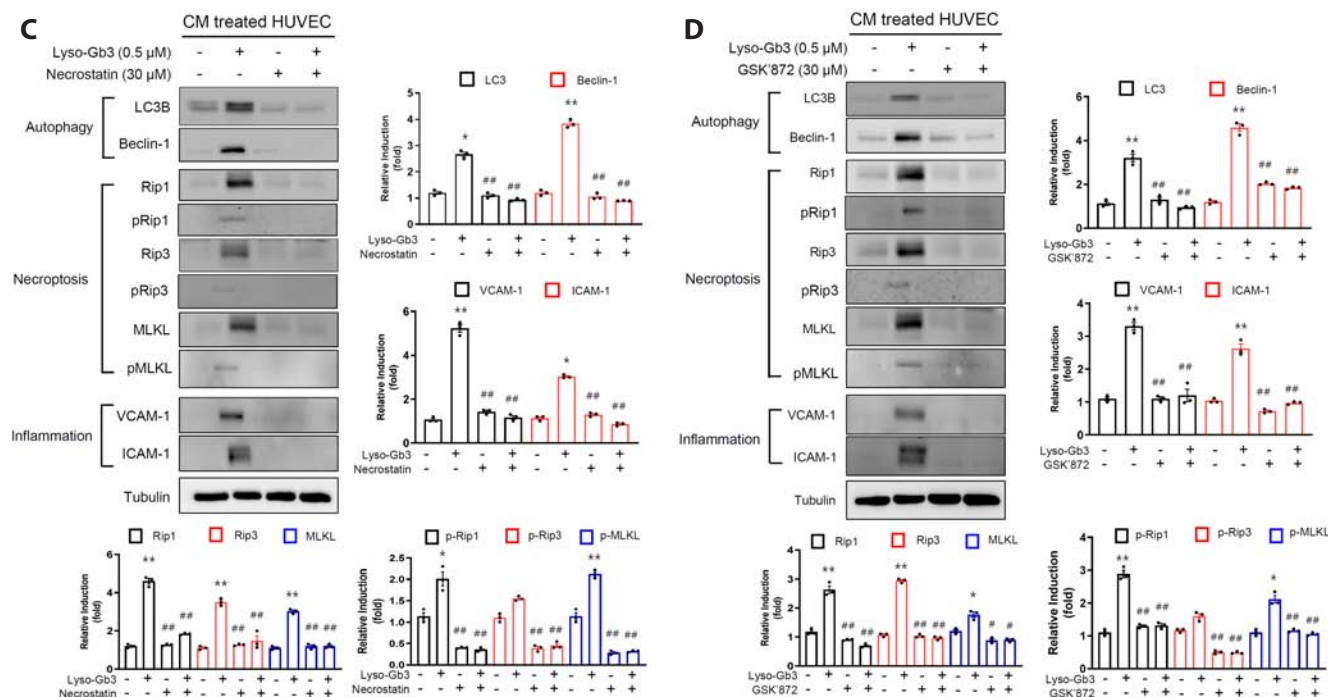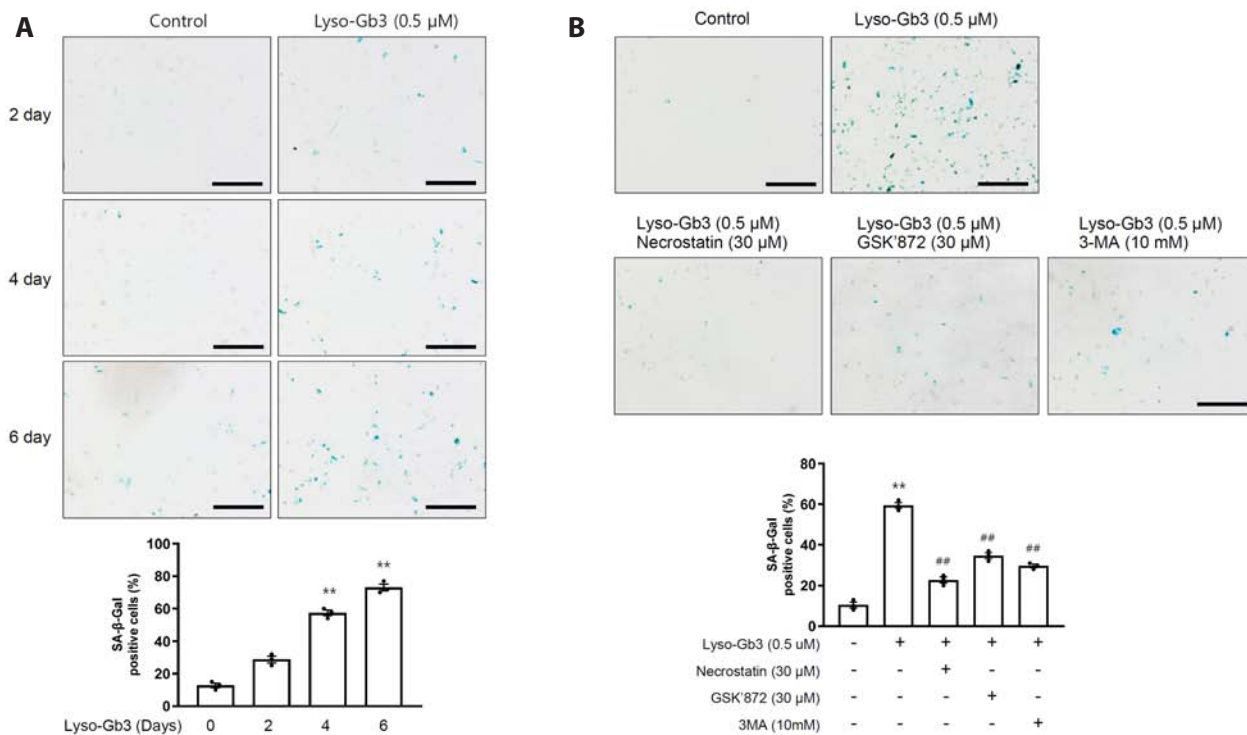
Fig. 3. Continued.

Fig. 4. Conditioned media from lyso-Gb3 treated ARPE-19 cells increases endothelial senescence. (A) Endothelial senescence was assessed by senescence-associated β-galactosidase (SA-β-Gal) staining in HUVECs treated with conditioned medium (CM) from lyso-Gb3 treated ARPE-19 cells. (B) The effects of necrostatin, GSK'872, or 3-MA on lyso-Gb3 treated ARPE-19 CM-induced HUVEC senescence as determined by SA-β-Gal assays. Images are representative of three independent experiments (B). Scale bar, 50 μm. Bar graphs show expressions as mean percentages of SA-β-Gal positive cells. 3-MA, 3-methyladenine; HUVEC, human umbilical vein endothelial cell. **p < 0.01 *vs.* vehicle control, ##p < 0.01 *vs.* lyso-Gb3 treated cells, one-way ANOVA followed by Bonferroni's *post-hoc* test.

GSK'872, or 3-MA significantly suppressed this staining (Fig. 4B). These results suggest that lyso-Gb3 induces retinal pigment epithelial cell-derived endothelial dysfunction *via* an autophagy-dependent necroptosis pathway in retinal layers in FD.

DISCUSSION

Gb3 accumulates in lysosomes during α-GalA deficiency, but the mechanisms of subsequent cellular dysfunction and ultimately, the symptoms of FD are not well understood [17]. Like other inherited glycosphingolipids, lipid-laden lysosomes can be associated to mitochondrial dysfunction in the fibroblasts of FD patients due to impaired autophagic flux, including mitophagy [18]. In addition, lyso-Gb3 is closely linked to podocyte loss and glomerular fibrosis in FD patients [19]. Here, we report lyso-Gb3 induces autophagy in ARPE-19 cells (a retinal pigment epithelial cell line), and that 3-MA (an autophagy-specific inhibitor) alleviated lyso-Gb3-induced necroptosis (Figs. 1 and 2). In addition, CM from lyso-Gb3 treated ARPE-19 cells induced endothelial inflammation and senescence in HUVECs (Figs. 3 and 4). These results indicate that lyso-Gb3 induces retinal pigment epithelial cell-derived endothelial dysfunction *via* an autophagy-dependent necroptosis pathway. The regulatory mechanism linking autophagy and necroptosis needs to be explored in further studies. Furthermore, RIP1 and RIP3 have been reported to play a role in reactive oxygen species (ROS) generation by increasing aerobic respiration [20], and we observed that lyso-Gb3-induced ROS generation was dependent on RIP3 (data not shown), which suggests ROS may be involved in lyso-Gb3-induced necroptosis and subsequent inflammatory responses.

Necroptosis is a newly identified form of programmed cell death that combines features of necrosis and apoptosis. Increasing evidence suggests the involvement of necroptosis in various diseases, including atherosclerosis [5], and in diabetic cardiac injury [21]. However, the roles of necroptosis in lyso-Gb3-induced vascular endothelial injury and the mechanism responsible for the protection afforded by exogenous necroptosis-associated inhibitors are unclear. Necrosis is proinflammatory process as it results in passive leakage of DAMPs caused by cytoplasmic membrane rupture [22]. The discovery of necroptosis, a regulated necrotic cell death mechanism, raised the possibility that there may be a program activated by the passive release of intracellular contents that promotes necroptosis-related inflammation. Many of the genes upregulated during necroptosis, such as those encoding inflammatory cytokines, are also upregulated during inflammation-associated processes, though they are more substantially upregulated during necroptosis [23]. These observations suggest that necroptosis might enhance lyso-Gb3-induced gene expression for inflammatory responses.

Interestingly, lyso-Gb3 treatment slightly increased rather than decreased cell viability despite the significant induction of necroptosis-related marker proteins (Fig. 1), which suggests that the lyso-Gb3-induced autophagy-dependent necroptosis pathway triggers inflammation but not cell death. It has been established that membrane-associated MLKL induces inflammatory responses in neighboring regions by causing membrane pore formation resulting in the release of intracellular DAMPs [24]. It is also known that RIP1 and RIP3 have non-necroptotic functions for inflammatory cytokine induction [25]. In addition, it has been reported that crosstalk between necroptosis and pyroptosis mediates inflammatory responses *via* MLKL-dependent NLRP3-mediated IL-1β secretion [26]. However, the role played by the RIP1/RIP3/MLKL cascade in lyso-Gb3-induced inflammatory responses *via* the autophagy-dependent necroptosis pathway has yet to be determined.

Inflammatory responses induce endothelial dysfunction characterized by impaired endothelial-dependent vasodilation that can lead to the development of vascular inflammatory diseases, such as atherosclerosis [27]. Several studies have suggested that aging is an independent risk factor for the development of cardiovascular diseases (CVDs) [28], and studies have demonstrated that cellular senescence increases the risk of CVDs. Accordingly, we investigated whether CM of lyso-Gb3 treated ARPE-19 might induce necroptosis, inflammation, and senescence phenotypes in HUVECs. Our results showed that CM of lyso-Gb3 treated ARPE-19 elicited endothelial necroptosis, inflammation, and senescence *via* the autophagy-dependent necroptosis pathway in HUVECs (Figs. 3 and 4). The suppression of endothelial inflammation and senescence by necroptosis inhibitors indicates epithelial necroptosis might be required for the triggering of the inflammatory interaction between epithelial and endothelial cells, and suggests, targeting the RIP1-RIP3-MLKL pathway offers a potential novel therapeutic means of addressing endothelial senescence-associated CVDs.

In conclusion, our study suggests a novel regulatory mechanism, whereby the autophagy-dependent necroptosis pathway-mediated enhancement of endothelial inflammation and senescence induced by lyso-Gb3 contributes to the pathogenesis of FD, and that therapeutic intervention *via* necroptosis inhibition may provide a novel therapeutic means of targeting the endothelial dysfunction-related complications of FD.

FUNDING

ACKNOWLEDGEMENTS

CONFLICTS OF INTEREST

The authors declare no conflicts of interest.

REFERENCES

1. Brady RO, Gal AE, Bradley RM, Martensson E, Warshaw AL, Laster L. Enzymatic defect in Fabry's disease. Ceramidetrihexosidase deficiency. *N Engl J Med.* 1967;276:1163-1167.

2. Lücke T, Höppner W, Schmidt E, Illsinger S, Das AM. Fabry disease: reduced activities of respiratory chain enzymes with decreased levels of energy-rich phosphates in fibroblasts. *Mol Genet Metab.* 2004;82:93-97.

3. Levine B, Klionsky DJ. Development by self-digestion: molecular mechanisms and biological functions of autophagy. *Dev Cell.* 2004;6:463-477.

4. Choi ME, Price DR, Ryter SW, Choi AMK. Necroptosis: a crucial pathogenic mediator of human disease. *JCI Insight.* 2019;4:e128834.

5. Pasparakis M, Vandenabeele P. Necroptosis and its role in inflammation. *Nature.* 2015;517:311-320.

6. Vitner EB, Salomon R, Farfel-Becker T, Meshcheriakova A, Ali M, Klein AD, Platt FM, Cox TM, Futerman AH. RIPK3 as a potential therapeutic target for Gaucher's disease. *Nat Med.* 2014;20:204-208.

7. Rodier F, Campisi J. Four faces of cellular senescence. *J Cell Biol.* 2011;192:547-556.

8. Nigro P, Abe J, Woo CH, Satoh K, McClain C, O'Dell MR, Lee H, Lim JH, Li JD, Heo KS, Fujiwara K, Berk BC. PKCzeta decreases eNOS protein stability via inhibitory phosphorylation of ERK5. *Blood.* 2010;116:1971-1979.

9. Debacq-Chainiaux F, Erusalimsky JD, Campisi J, Toussaint O. Protocols to detect senescence-associated beta-galactosidase (SA-betagal) activity, a biomarker of senescent cells in culture and in vivo. *Nat Protoc.* 2009;4:1798-1806.

10. El-Awady AR, Miles B, Scisci E, Kurago ZB, Palani CD, Arce RM, Waller JL, Genco CA, Slocum C, Manning M, Schoenlein PV, Cutler CW. Porphyromonas gingivalis evasion of autophagy and intracellular killing by human myeloid dendritic cells involves DC-SIGN-TLR2 crosstalk. *PLoS Pathog.* 2015;10:e1004647.

11. Zhang JM, An J. Cytokines, inflammation, and pain. *Int Anesthesiol Clin.* 2007;45:27-37.

12. Hanada T, Yoshimura A. Regulation of cytokine signaling and inflammation. *Cytokine Growth Factor Rev.* 2002;13:413-421.

13. Chan AH, Schroder K. Inflammasome signaling and regulation of interleukin-1 family cytokines. *J Exp Med.* 2020;217:e20190314.

14. van Eijk M, Ferraz MJ, Boot RG, Aerts JMFG. Lyso-glycosphingolipids: presence and consequences. *Essays Biochem.* 2020;64:565-578.

15. Rozenfeld P, Feriozzi S. Contribution of inflammatory pathways to Fabry disease pathogenesis. *Mol Genet Metab.* 2017;122:19-27.

16. Sanchez-Niño MD, Carpio D, Sanz AB, Ruiz-Ortega M, Mezzano S, Ortiz A. Lyso-Gb3 activates Notch1 in human podocytes. *Hum Mol Genet.* 2015;24:5720-5732.

17. Ferraz MJ, Kallemeijn WW, Mirzaian M, Herrera Moro D, Marques A, Wisse P, Boot RG, Willems LI, Overkleeft HS, Aerts JM. Gaucher disease and Fabry disease: new markers and insights in pathophysiology for two distinct glycosphingolipidoses. *Biochim Biophys Acta.* 2014;1841:811-825.

18. Stepien KM, Roncaroli F, Turton N, Hendriksz CJ, Roberts M, Heaton RA, Hargreaves I. Mechanisms of mitochondrial dysfunction in lysosomal storage disorders: a review. *J Clin Med.* 2020;9:2596.

19. Sanchez-Niño MD, Sanz AB, Carrasco S, Saleem MA, Mathieson PW, Valdivielso JM, Ruiz-Ortega M, Egido J, Ortiz A. Globotriaosylsphingosine actions on human glomerular podocytes: implications for Fabry nephropathy. *Nephrol Dial Transplant.* 2011;26:1797-1802.

20. Yang Z, Wang Y, Zhang Y, He X, Zhong CQ, Ni H, Chen X, Liang Y, Wu J, Zhao S, Zhou D, Han J. RIP3 targets pyruvate dehydrogenase complex to increase aerobic respiration in TNF-induced necroptosis. *Nat Cell Biol.* 2018;20:186-197.

21. Cougnoux A, Cluzeau C, Mitra S, Li R, Williams I, Burkert K, Xu X, Wassif CA, Zheng W, Porter FD. Necroptosis in Niemann-Pick disease, type C1: a potential therapeutic target. *Cell Death Dis.* 2016;7:e2147.

22. Zhu K, Liang W, Ma Z, Xu D, Cao S, Lu X, Liu N, Shan B, Qian L, Yuan J. Necroptosis promotes cell-autonomous activation of proinflammatory cytokine gene expression. *Cell Death Dis.* 2018;9:500.

23. Zu R, Yu Z, Zhao J, Lu X, Liang W, Sun L, Si C, Zhu K, Zhang T, Li G, Zhang M, Zhang Y, Liu N, Yuan J, Shan B. Quantitative analysis of phosphoproteome in necroptosis reveals a role of TRIM28 phosphorylation in promoting necroptosis-induced cytokine production. *Cell Death Dis.* 2021;12:994.

24. Kaczmarek A, Vandenabeele P, Krysko DV. Necroptosis: the release of damage-associated molecular patterns and its physiological relevance. *Immunity.* 2013;38:209-223.

25. Jung S, Seo DJ, Yeo D, Wang Z, Min A, Zhao Z, Song M, Choi IS, Myoung J, Choi C. Experimental infection of hepatitis E virus induces pancreatic necroptosis in miniature pigs. *Sci Rep.* 2020;10:12022.

26. Frank D, Vince JE. Pyroptosis versus necroptosis: similarities, differences, and crosstalk. *Cell Death Differ.* 2019;26:99-114.

27. Godo S, Shimokawa H. Endothelial functions. *Arterioscler Thromb Vasc Biol.* 2017;37:e108-e114.

28. Rodgers JL, Jones J, Bolleddu SI, Vanthenapalli S, Rodgers LE, Shah K, Karia K, Panguluri SK. Cardiovascular risks associated with gender and aging. *J Cardiovasc Dev Dis.* 2019;6:19.